ACS APPLIED MATERIALS & INTERFACES

Research Article

www.acsami.org

Efficient Heterogeneous Catalytic Hydrogenation of Acetone to Isopropanol on Semihollow and Porous Palladium Nanocatalyst

Aamna Balouch,[†,‡] Akrajas Ali Umar,*[,†] Athar Ali Shah,[†] Muhamad Mat Salleh,[†] and Munetaka Oyama[§]

[†]Institute of Microengineering and Nanoelectronics, Universiti Kebangsaan Malaysia, 43600 UKM Bangi, Selangor, Malaysia

[§]Department of Material Chemistry, Graduate School of Engineering, Kyoto University, Nishikyo-ku, Kyoto 615-8520, Japan

ABSTRACT: Highly efficient and remarkable selective acetone conversion to isopropanol has been achieved via a heterogeneous catalytic hydrogenation of acetone by $NaBH_4$ in the presence of semihollow palladium nanoparticles (PdNPs) grown on ITO substrate. PdNPs with high surface defect grown on an indium tin oxide (ITO) surface were prepared via a simple immersion of the substrate into a solution containing K_2PdCl_6, sodium dodecyl sulphate (SDS), and formic acid for 2 h at room temperature. The sample showed remarkably high heterogeneous catalytic efficiency by producing 99.8% of isopropanol within 6 min using only 0.28 μg of PdNPs on the ITO surface. The present system exhibits heterogenenous catalytic hydrogenation efficiency 1×10^6 time higher than using the conventional Raney Ni system.

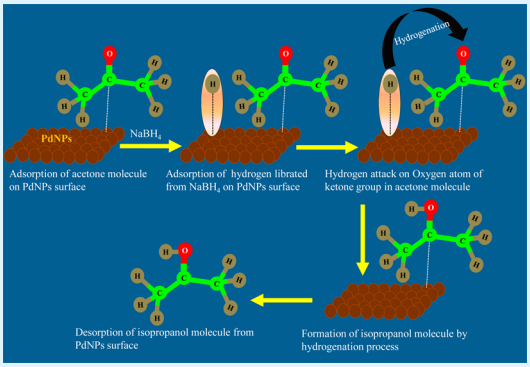

KEYWORDS: *hydrogenation of acetone, semihollow, Porous, Pd nanocatalyst, LPD method*

1. INTRODUCTION

Isopropanol is in high demand in direct isopropanol (2-propanol) (DIPA) fuel cells because of their high energy production, much lower crossover current, ease to oxidize, production of more hydrogen, and being less toxic than other alcohols such as methanol and ethanol.[1] Apart from its promising application in the DIPA fuel cell, the production of isopropanol is expensive, time consuming, and produces a toxic by-product. The efforts towards the production of isopropanol with an efficient but green method should be continuously demonstrated.

Acetone hydrogenation is a cheap and environmentally safe alternative method for the production of isopropanol because of its easy reduction of C═O to convert into C−OH.[2,3] The basic hydrogenation process of crude acetone uses Raney nickel or a mixture of copper and chromium oxide as the catalyst. However, despite its high efficiency this process is only useful when being coupled with the Cumene process,[2] which is a tedious and complicated multiple-step process. As this approach also produces an explosive intermediate (cumene hydroperoxide) and benzene contamination, as well as the use of a corrosive catalyst, it has a high impact on the environment.[4] Recently, a straightforward process that uses metal supported "semi" heterogeneous catalysts (because of using microscale support), such as Pd on silica, Au and Pt on Al_2O_3, Pt on SiO, Pt on TiO microspheres and Cu, Pt, Pd, and Rh on Kieselghur, the hydrogenation of acetone to isopropanol has been reported.[5−8] However, they have one main disadvantage: the use of a high temperature process that in many cases can be up to 250 °C. Moreover, this approach has a complicated experimental procedure that results in high costs and is time consuming. The use of unsupported Pt, Ni, Fe, and W catalysts has also been demonstrated for acetone hydrogenation. Although these methods are the most efficient for the hydrogenation of acetone, they are not selective and produce low molecular weight hydrocarbons (C_1−C_4).[7,9,10]

Here, we demonstrate highly efficient heterogeneous catalytic and excellent selectivity properties for the hydrogenation of acetone to isopropanol using semihollow and porous Pd nanostructure grown on ITO substrate. Despite Pd nanoparticles having been widely used as catalysts for C−C coupling reactions, such as Mizoroki− Heck, Suzuki−Miyaura and Sonogashira reactions,[11−21] and the hydrogenation of unsaturated alkenes, alkyne and olefins,[22−26] the use of Pd nanoparticles for hydrogenation of acetone to isopropanol has not yet been demonstrated. Here, by simple synthesis the Pd nanostructure with a hollow and a high porous morphology directly on ITO substrate, high efficiency, and selectivity acetone hydrogenation to isopropanol with a yield of up to approximately 99% within a short reaction time can be achieved. Because of its simple preparation procedure and rapid hydrogenation process, as well as a heterogeneous process with no possible catalyst contamination, the semihollow PdNPs can be potentially used as a green approach for efficient isopropanol production. By also considering the unique morphology of the present PdNPs and the special optical property of Pd nanostructure, the PdNPs with such semihollow

Received: July 31, 2013
Accepted: September 11, 2013
Published: September 11, 2013

Table 1. Comparison of the Efficiency of PdNP Nanocatalyst for Acetone Hydrogenation with Reported Results of Other Metal Catalysts

sample no.	catalyst	mass of catalyst	temp (°C)	conversion (%)	selectivity (%)	conversion efficiency	reference
1	Pd	0.702 μg	28	99.8	100	28% μg^{-1} M^{-1}	present work[a]
2	NiO, CoO_4	0.5 g	200	50	100	2.5% g^{-1} $°C^{-1}$	8b
3	Co/Al_2O_3	0.5 g	200	64	80	3.2% g^{-1} $°C^{-1}$	8b
4	Raney Ni	2.9 g	80	99.92	100	72.69% g^{-1} $°C^{-1}$	44b
5	Raney cobalt	7.8 g	120	82.5	99	67.31% g^{-1} $°C^{-1}$	44b

[a]$NaBH_4$ is used as hydrogen source. [b]Temperature is used along with hydrogen gas purging.

structure should also be potentially used for enhanced-performance in optoelectronic[27] and nonlinear optical.[28,29]

2. EXPERIMENTAL SECTION

Synthesis of Porous Palladium Nanoparticles on ITO Substrate. Palladium NPs on the ITO surface were prepared using a Liquid Phase Deposition method, namely hydrolysis of Pd-complex in the presence of formic acid at ambient temperature. In a typical procedure, the growth of Pd NPs on the substrate was carried by immersing a clean ITO substrate (sheet resistance of 9−22 Ω per square, purchased from a VinKarola instrument, USA) that has been washed by consecutive ultrasonication in acetone and ethanol for 30 min. It was then placed into a 15 mL growth solution that contains 0.5 mM potassium hexachloro palladate (Fluka), 10 mM Sodium dodecylesulfate (Fluka) and 1.0 mM Formic acid (Fluka). The solution was continuously stirred during the growth process. The growth time and temperature are 2 h and room temperature ca. 25 °C, respectively. Then the sample was removed from the growth solution, rinsed with a copious amount of deionized water, and dried with a flow of nitrogen gas.

All chemicals were used as received without any further purification. All of the chemicals were prepared in aqueous solution using pure water obtained from a Milli-Q water purification system.

Field emission scanning electron microscopy (FESEM) (Zeiss Supra 55VP FE SEM model) with resolution of 1.0 nm at 30 kV and transmission electron microscopy (TEM) (model Philips CM 12 TEM) with resolution of varying from 1.4 to 4 A° at 120 kV were used to study the morphology and the structure of the nanoparticle. The X-ray diffraction (XRD) experiment was carried out using the XRD Bruker D8 system with a CuKα irradiation and a scanning rate of 0.025°/s.

Heterogeneous Catalysts for Hydrogenation of Acetone. The catalytic property of the porous PdNPs was evaluated by the hydrogenation reaction of acetone using sodium borohydride. In a typical procedure, ITO substrate decorated porous PdNPs were immersed into a glass vial containing 15 mL of mixed-aqueous solution of 0.05 mol L^{-1} acetone and 1.0×10^{-4} mol L^{-1} sodium borohydride. The solution was continuously stirred at a constant speed (ca. 400 rpm) during the reaction. To obtain the catalytic effect of the PdNPs in the hydrogenation of acetone, we recorded absorption spectrum of the solution every 5 min by taking a portion of the solution (approximately 3 mL). The solution was transferred into a quartz cuvet for absorption spectrum measurement using a Perkin-Elmer Lambda 900 UV−visible−NIR spectrophotometer. The resolution for UV/Vis and NIR of this instrument are <0.05 nm and <0.20 nm, respectively. The hydrogenation reaction was evaluated for 10 min.

To confirm the formation of isopropanol in the hydrogenation of acetone, we carried out a gas chromatography analysis. A gas chromatography instrument (Agilent 5890 series II) equipped with a flame ionization detector (FID) was used. The instrument is equipped with an analytical column of DB-5HT capillary column with dimensions of 30 m × 0.25 mm (inner diameter) and a 0.1 μm film thickness. Helium was used as the carrier gas. The instrument was operated under a temperature range of 50-200 °C with a ramp rate of 4 °C/min. The injector and detector temperatures were set at 210 °C and 295 °C, respectively. To evaluate the efficiency of the system with respect to amount of catalyst used and then compare it with the recently reported results, we calculated the mass of particles on the ITO substrate. By using the density of palladium of 1.2023×10^{-11} g μm^{-3}, the average volume of a single particle of 6.54×10^{-5} μm^3 (diameter = 50 nm), and by using the relation $m = DV$, where m, D and V are corresponding to mass, mass density and nanoparticle volume, we obtained the mass of a single particle of 7.85×10^{-16} g. Because the surface density of palladium NPs on the ITO surface (from FESEM image analysis) of 500 particles/μm^2, the mass of the palladium nanocatalyst on the substrate area of 1.5 × 1.2 cm^2 (one ITO slide sample) is approximately 0.7 μg. The efficiency was then calculated using the relation:

$$\eta = \frac{\%_{\text{yield}}}{\text{mass of particle} \times \text{mM of } NaBH_4} \quad (1)$$

where $\%_{\text{yield}}$ is the percentage of isopropanol production. The efficiency of the present system and the recently reported results are summarized in Table 1.

To determine the yield of isopropanol after a catalytic hydrogenation, we first plotted the standard optical absorption calibration graph for acetone in the range of 0.01−0.1 mol L^{-1} at the peak wavelength of 265 nm against water as a reagent blank. A straight line of $y = mx + C$, with y, m, x, and C having absorbance at the centre band, slope of the graph, concentration and intersection point with y-axis, respectively, was interpolated from the calibration data. Figure 1 shows

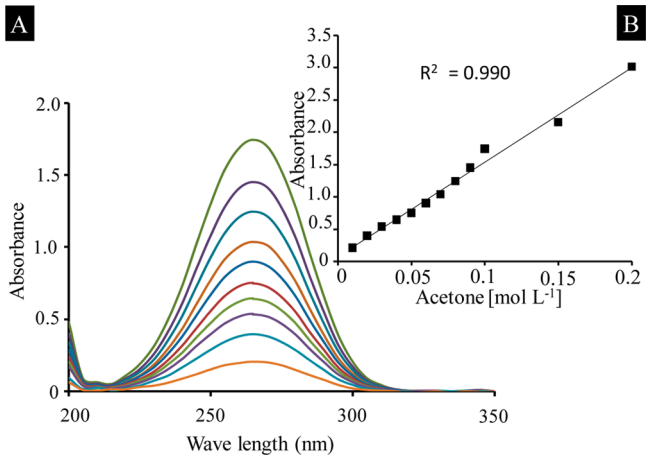

Figure 1. (A) Optical absorption spectra for acetone with varying concentration from 0.01−0.1 mol L^{-1}. (B) is the standard calibration graph of acetone that is plotted from the absorbance at the centre of absorption band.

typical optical absorption calibration data for acetone obtained in this study. The yield of isopropanol was then obtained from the change of acetone concentration calculated using the relation

$$\frac{C_i - C_f}{C_i} \times 100 \quad (2)$$

where C_i and C_f are the initial and final concentrations of acetone.

3. RESULTS AND DISCUSSION

Semihollow and porous palladium nanoparticles were successfully grown on ITO substrate following our recently reported method,[30−37] which was for direct growth of a nanostructure on the solid substrate using the solution or liquid phase deposition method. This used a growth solution containing a mixed aqueous solution of 0.5 mM K_2PdCl_6, 10 mM sodium dodecylsulfate, and 1.0 mM formic acid. In the typical preparation procedure, during the reaction, the growth solution's color changed from dark brown to light brown with the addition of formic acid. The solution color then gradually decreased and became completely transparent at the reaction time of around 2 h. At this stage, a uniform black film was observed on the ITO surface, reflecting the formation of Pd nanostructure growth on the surface. Surprisingly, no attachment was observed on the glass container, which infers that the growth of palladium is selective only on the ITO surface. The photograph of the solution evolution during this process is shown in Figure 2A.

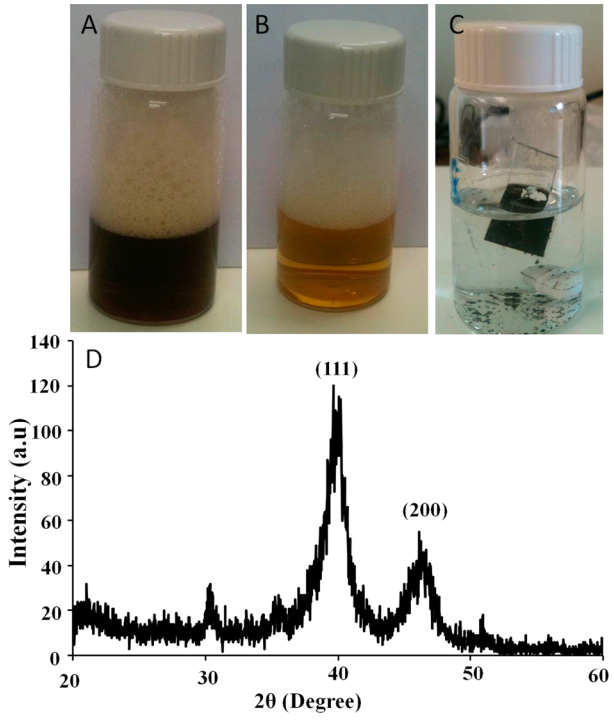

Figure 2. (A) Photograph of initial growth solution that contains 0.05 mM of K_2PdCl_6 and 10.0 mM of SDS. Then, (B) after the addition of 1.0 mM formic acid and (C) the reaction condition after finishing the reaction for 2 h, Black Pd film is observed on the ITO surface. (D) Typical XRD spectrum of the PdNPs.

The formation of the Pd nanostructure on the surface was confirmed by X-ray diffraction analysis on the as prepared sample, and the results are shown in Figure 2B. As can be seen from the figure, two main peaks appear in the spectrum at the 2θ of 38.38 and 45.15. This diffraction spectrum was found to agree well with JCPDS card No. 05-0681 (the powder diffraction file (PDF) for fcc Pd crystal), whose peaks at 2θ = 38.38 and 45.15 are associated with the (111) and (200) planes, respectively. This result confirms the effectiveness of the present approach to grow PdNPs directly on the substrate surface from the solution phase.

Figure 3 shows the typical FESEM image of the PdNPs on the substrate surface prepared using this approach. As Figure 3

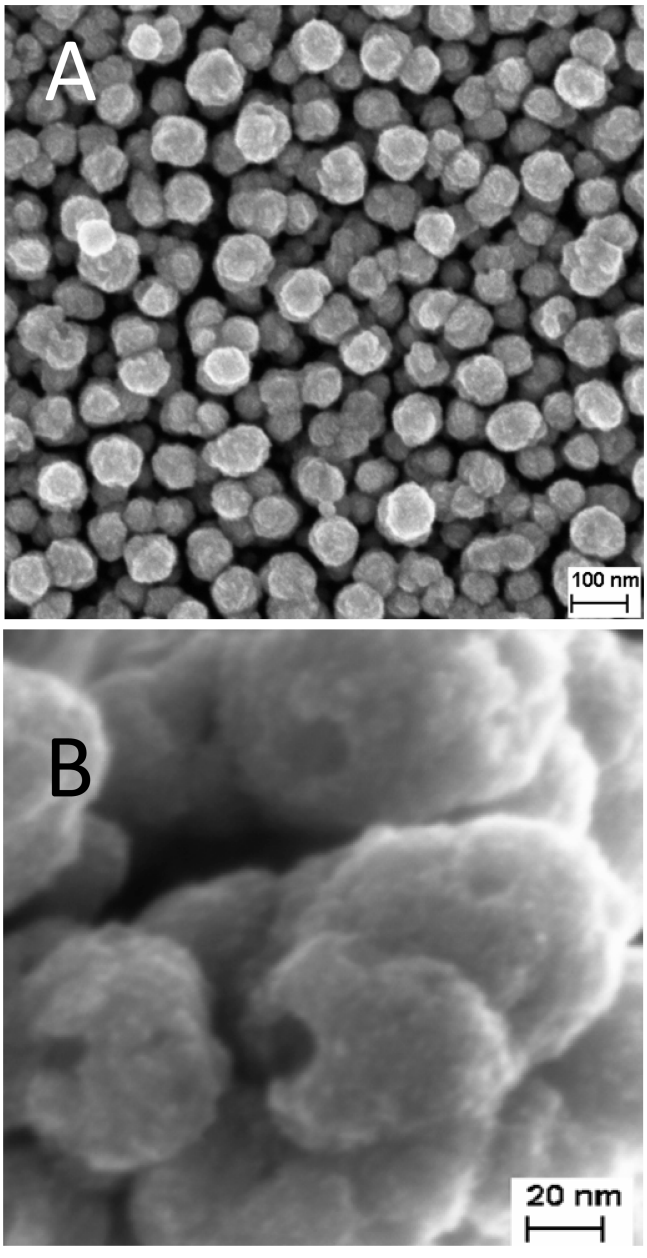

Figure 3. Typical FESEM image of PdNPs grown on ITO substrate. (A) Low- and (B) high-magnification FESEM images, respectively.

shows a high-density, close-packed spherical-like nanostructure is obtained on the surface. The nanostructure was also found to homogeneously cover almost 90% of the substrate surface with the particle distribution of 500 ± 20 particles per um^2. With the presence of a large scale air gap amongst the nanoparticles, the surface exhibits a highly porous property. This structure may be good for enhanced catalytic reaction. The diameter of the PDNPs is in the range of 50−70 nm, adopting the Gaussian-like distribution. The morphology of the PdNPs was further characterized by high resolution FESEM analysis. It was found that the PdNPs compose a semihollow structure with hollow depths varying from 10 to 20 nm. In addition to these unique properties, the semihollow PdNPs exhibit the surface containing dotted-rough, porous and hilly surface structures.

TEM analysis on the sample indicated that the PdNPs resemble a spongy structure that is constructed by smaller crystallite aggregates rather than a solid structure (see Figure 4B). The

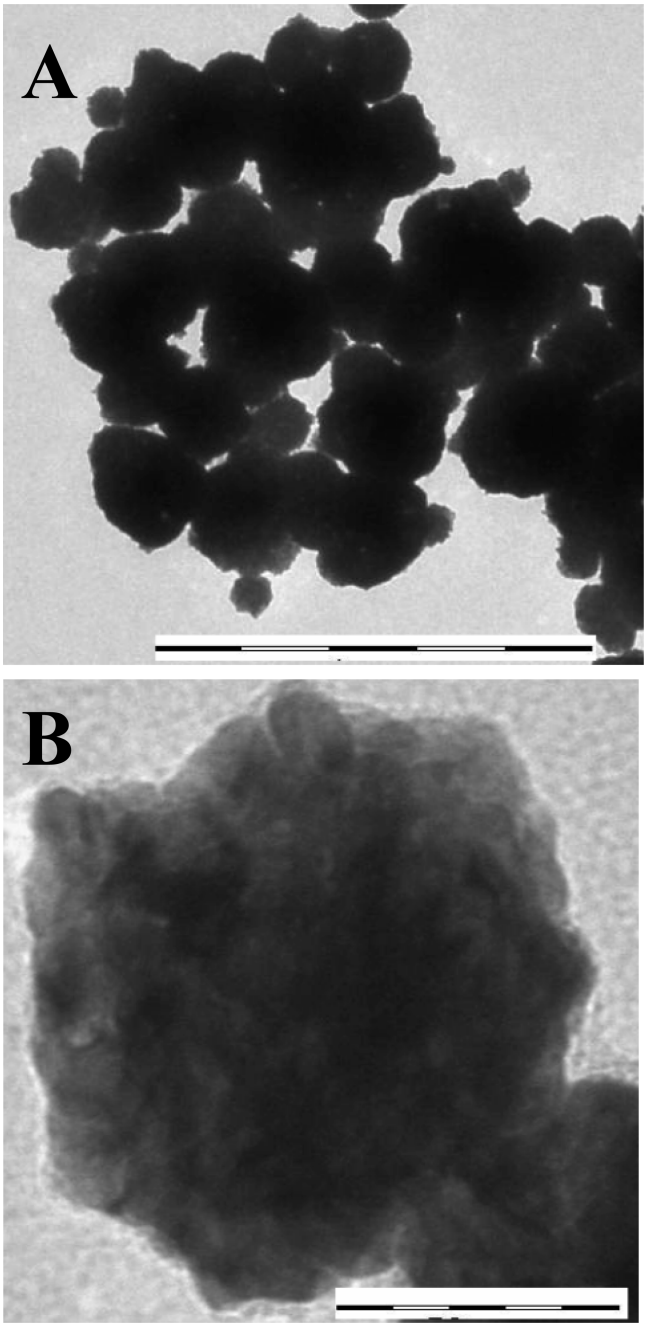

Figure 4. Typical TEM images of PdNPs in (A) low and (B) high resolutions. Scale bars are (A) 1 μm and (B) 50 nm.

nanoparticles with a semihollow shape may act as a microreactor and offer greatly enhanced efficiency as a catalyst because of their porous, defected, dotted, hilly, and spongy structure. This condition may facilitate enhanced mobility of charge carriers to different reaction positions and a more effective reaction process. Thus, enhanced catalytic properties are expected from these nanostructures.

The formation of semihollow PdNPs on the substrate surface is assumed as the effective combinative effect of surfactant and reducing agent used during the growth process. Especially with the reductant, the use of formic acid is crucial for the formation of a hollow structure. The use of other reducing agents, such as ascorbic acid, may only produce spherical and cubic or nanobrick morphology.[38] In the present study, formic acid is predicted to produce an acidic effect in the reaction media, which in turn will induce an etching or oxidation phenomenon to the grown nanostructure. The depth of the hollow is then related to the acidic nature of the solution and decreases when growth time increases. At a particular condition at which the acidic nature is weak, the oxidation is stopped and a semihollow nanoparticle forms. However, in the present stage the crystal plane involved in the oxidation process is not yet known. Nevertheless, by considering the surface energy of Pd fcc crystals, a high energy and less stable surface of (110) might be the most easiest plane to be oxidized.[39]

The effect of nanocluster aggregation in the formation of bigger PdNPs could also be considered as a factor for the formation of a hollow structure.[40] Because the reduction of Pd ion always produces a small cluster in the solution instead of supporting the growing plane on the substrate, they tend to aggregate each other in the effort to minimize their high surface energy. Unoriented aggregation may produce a porous and hollow structure. Such cluster aggregation is confirmed from the TEM image (see Figure 4).

On the effective and selective growth of PdNPs on the ITO surface, the electrostatic interaction between the negatively charged nanoparticles and positively charged ITO surface can be considered as the driving factor for the formation of high density PdNP growth on the surface. It is predicted that the Pd cluster are favored to form in a solution (instead of nucleates) on the surface at the beginning of the reaction. The negative head group of SDS surfactant may encapsulate the Pd nanocluster and then attach them to the positively charged ITO surface (as the presence of electropositive In and Sn) via electrostatic interaction, which promotes the growth of bigger PdNPs. Thus, this condition facilitates high density growth of PdNPs on the ITO substrate surface.

Heterogeneous Catalytic Hydrogenation of Acetone to Isopropanol. Heterogeneous catalytic properties of the new pd structure have been evaluated in hydrogenation of acetone to produce isopropanol. In the typical procedure, we mixed 50 mmol L^{-1} acetone and 0.5 mmol L^{-1} of $NaBH_4$, and the hydrogenation of acetone was monitored by UV−visible spectrophotometry in the presence and absence of the PdNPs catalyst. Hydrogenation was determined by a decrease in the absorbance (hypochromic effect) and blue-shifting (hypsochromic effect) on the acetone peak at 265 nm. The hypo- and hypsochromic effect revealed a reduction of concentration of acetone and selective formation of isopropanol, respectively, by sodium borohydride.[8,41]

Prior to evaluating the catalytic hydrogenation of acetone by PdNPs, we examined the optimum $NaBH_4$ concentration used in the hydrogenation process (i.e., the value where the reduction of acetone is saturated), in the absence of a palladium catalyst, by varying the concentration from 0.1 to 20 mmol L^{-}. Figure 5A shows typical UV−visible spectra of acetone under variation of $NaBH_4$ concentration from 0.1 to 20 mmol L^{-1}. From the figure, it can be seen that there is a drastic decrease in the absorbance rate at the wavelength of 265 nm when $NaBH_4$ concentration increases from 0.1 to 0.5 mmol L^{-1}. However, only a small change was observed if the $NaBH_4$ concentration further increased, even up to 20 mmol L^{-1}. From the absorption profile, we know that the isopropanol is formed

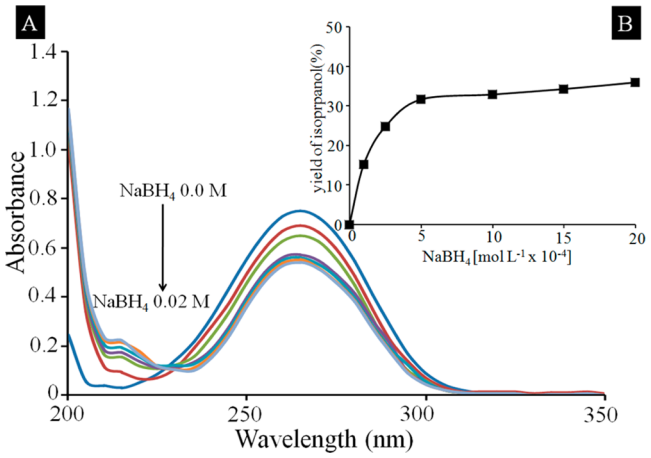

Figure 5. (A) UV–vis spectra and (B) the plot for catalytic hydrogenation dynamic of acetone to IPA by varying the concentration of $NaBH_4$ in the range of 0.1–2 mM and at a fixed concentration (0.05 M) of acetone in absence of PdNPs, respectively.

during the reaction, judging from the hypso- and hypochromic characters in the absorption spectrum. The yield at $NaBH_4$ of 0.5 mmol L^{-1} is as high as 33% and it increases only around 2–3% if the concentration of $NaBH_4$ further increases. Despite $NaBH^-_4$ being the hydrogen source for acetone hydrogenation, the limited increase in the hydrogenation process as their concentration increases can be associated with the possibility of steric effect arising because of oversaturation of $NaBH^-_4$ that hinders further hydrogenation. Therefore, the catalyst is required to further enhance the hydrogenation process. To evaluate the catalytic properties of our new PdNPs in the hydrogenation of acetone, the $NaBH_4$ concentration of 0.5 mmol L^{-1} was selected, i.e., the optimum point where limited steric effect was expected.

Next, we examine the hydrogenation of acetone in the presence of the palladium nanocatalyst. Figure 6 shows the

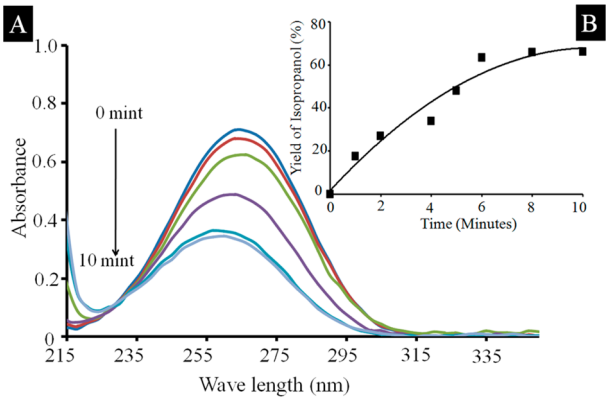

Figure 6. (A) Optical absorption and (B) heterogeneous catalytic hydrogenation kinetics of acetone in the presence of PdNPs.

dynamic heterogeneous catalytic hydrogenation of acetone by PdNPs in the presence of 0.5 mM $NaBH^-_4$ within the reaction time of up to 10 min. As Figure 6 shows, the absorbance at the peak wavelength effectively decreases with an increase in the reaction time. By considering the absorption spectrum properties of the acetone during the reaction that shows both intense hypso- and hypochromic characters, we believe that effective isopropanol formation is expected and its yield linearly increases with an increase in the reaction time. However, it was found to be saturated after the reaction time reached 6 min (see Figure 6B). This could be due to the consumption of hydrogen for acetone reduction provided from the $NaBH_4$. The yield of isopropanol as high as 60% was obtained for the reaction time of 6 min. This yield is much higher compared to those shown in Figure 5, i.e., without the PdNPs catalyst. Thus, this confirms the excellent heterogeneous catalytic properties of PdNPs. A gas chromatography analysis of the product interestingly revealed that the product is isopropanol without the presence of any other by-product, reflecting the high selectivity of the heterogeneous catalytic hydrogenation of acetone utilizing semihollow PdNPs.

To improve the yield of isopropanol by complete hydrogenation/reduction of acetone, we optimized the catalyst dose in the reaction while keeping the concentration of $NaBH_4$ and acetone unchanged. The catalyst dose was increased by adding up to 4 slides of PdNPs-coated ITO substrate into the reaction. It was found that the yield of isopropanol linearly increased with an increase in the number of slides involved in the reaction. In the typical process, the yield of isopropanol increased from 66% to 73, 81, and 99.8% when 2, 3, and 4 slides, respectively, were introduced in the reaction. This confirmed an extremely effective heterogenous catalytic hydrogenation of acetone. The result for the heterogeneous catalytic hydrogenation of acetone in the presence of multiple PdNPs-coated ITO substrates is presented in Figure 7.

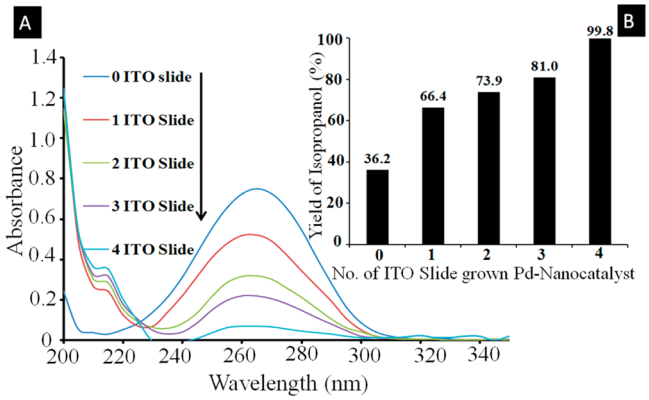

Figure 7. (A) Heterogeneous catalytic hydrogenation of acetone and (B) the yield of isopropanol using multiple PdNPs-coated ITO slides at a fixed concentration of 0.05 M acetone and 0. 5 mM $NaBH_4$.

As previously mentioned in the Experimental Section, to obtain the catalytic hydrogenation efficiency of our system and to compare with previous results we calculated the concentration of PdNPs-coated ITO substrate in the reaction. In the typical result, the concentration of the catalyst when using a single PdNPs-coated ITO slide of dimension 1.5 × 1.2 cm^2 is 0.07 μg/mL or approximately 0.28 μg/mL if using 4 PdNPs-coated ITO slides. By considering the yield of isopropanol of 99.8% if using 4 slides containing PdNPs, the heterogeneous catalytic hydrogenation efficiency per micrograms of catalyst and mol of $NaBH_4$ used is as high as 28%. This result is 1×10^6 orders higher than the recently reported results. The comparison of the performance of the present system and the reported result are presented in Table 1. Because the process is heterogeneous in nature and operates at room temperature, the semihollow PdNPs system should become a potential

dx.doi.org/10.1021/am403087m | ACS Appl. Mater. Interfaces 2013, 5, 9843–9849

alternative for green and economic large-scale isopropanol production.

The efficient hydrogenation of acetone in the present PdNPs is assumed as the effective catalytic activity of PdNPs due to the semihollow shape with porous and spongy structure that provides a high surface area for dynamic surface interaction (absorption/desorption). When one mole of $NaBH_4$ is added into the acetone solution, 4 moles of hydrogen will be released. In the first step, the hydrogen and acetone are adsorbed on the PdNPs' surface to form a metal−hydrogen and metal−carbon bond.[42] Then, in the second step, the hydrogen will be transferred to the ketone carbon (C═O) of the attached acetone molecule forming C−OH. This process is followed by the carbon-pd bond breaking, which leads to the desorption of the alcohol product from the metal surface to the solution and creates a vacant space for the adsorption of the new molecule.[43] At this stage hydrogenation is completed. This whole reaction is very fast and completed within 5−8 min.

The high selectivity property of the present system can be associated with the effective catalysis process of semihollow PdNPs with unique surface energy that may facilitate the formation of isopropanol. The exact crystal plane that characterized the PdNPs is not yet clear. However, high-resolution transmission microscopy analysis is being pursued on this sample and the results will be presented in a different report.

4. CONCLUSION

High-efficiency hydrogenation of acetone to isopropanol has been demonstrated using semihollow palladium nanocatalyst grown on ITO substrate. In the typical process, the system may effectively convert the acetone to isopropanol with a yield as high as 99.8% for only within 6 min of the reaction time without producing any other by-product, which reflects the high selectivity of the system. The highly porous, highly surface defect, spongy and semihollow structure is considered a key factor for the high performance of the nanocatalyst for the heterogeneous process. With no side product and a room-temperature process, the semihollow PdNPs may be used as a green approach for production of isopropanol for fuel cells.

AUTHOR INFORMATION

Corresponding Author

*E-mail: akrajas@ukm.my.

Notes

The authors declare no competing financial interest.

‡A.B. is on leave from Center of Excellence in Analytical Chemistry, University of Sindh, Jamshoro, Pakistan

ACKNOWLEDGMENTS

This work was partially supported by the Universiti Kebangsaan Malaysia, the Ministry of Education and Ministry of Science, Technology and Innovation of Malaysia under research grant FRGS/1/2012/SG02/UKM/02/3, DIP-2012-16 and 03-01-02-SF0836. The authors acknowledge Mr. M. Hasnol Naim Abd. Hamid and Mr. Idris Sharif for the FESEM analysis.

REFERENCES

(1) Cao, D. X.; Bergens, S. H. *J. Power Sources* **2003**, *124*, 12−17.
(2) Papa, A. Propanols. In *Ullmann's Encyclopedia of Industrial Chemistry*; Wiley-VCH, Weinheim. Germany, 2005; DOI 10(14356007):a22_173.
(3) Sumodjo, P.; da Silva, E.; Rabockai, T. *J. Electroanal. Chem. Interfacial Electrochem.* **1989**, *271*, 305−317.
(4) Jing, S. B.; Wang, Z. L.; Zhu, W. C.; Guan, J. Q.; Wang, G. J. *React. Kinet. Catal. Lett.* **2006**, *89*, 55−61.
(5) Gandia, L.; Diaz, A.; Montes, M. *J. Catal.* **1995**, *157*, 461−471.
(6) Gandía, L. M.; Montes, M. *J. Mol. Catal.* **1994**, *94*, 347−367.
(7) Sen, B.; Vannice, M. A. *J. Catal.* **1988**, *113*, 52−71.
(8) Narayanan, S.; Unnikrishnan, R. *J. Chem. Soc., Faraday Trans.* **1998**, *94*, 1123−1128.
(9) Farkas, A.; Farkas, L. *J. Am. Chem. Soc.* **1939**, *61*, 3396−3401.
(10) Stoddart, C.; Kemball, C. *J. Colloid Sci.* **1956**, *11*, 532−542.
(11) Moreno-Mañas, M.; Pleixats, R. *Acc. Chem. Res.* **2003**, *36*, 638−643.
(12) Astruc, D.; Lu, F.; Aranzaes, J. R. *Angew. Chem., Int. Ed.* **2005**, *44*, 7852−7872.
(13) Li, Y.; Zhou, P.; Dai, Z.; Hu, Z.; Sun, P.; Bao, J. *New J. Chem.* **2006**, *30*, 832−837.
(14) Narayanan, R.; El-Sayed, M. A. *J. Am. Chem. Soc.* **2003**, *125*, 8340−8347.
(15) Gallon, B. J.; Kojima, R. W.; Kaner, R. B.; Diaconescu, P. L. *Angew. Chem., Int. Ed.* **2007**, *46*, 7251−7254.
(16) Niembro, S.; Shafir, A.; Vallribera, A.; Alibés, R. *Org. Lett.* **2008**, *10*, 3215−3218.
(17) Mennecke, K.; Cecilia, R.; Glasnov, T. N.; Gruhl, S.; Vogt, C.; Feldhoff, A.; Vargas, M. A. L.; Kappe, C. O.; Kunz, U.; Kirschning, A. *Adv. Synth. Catal.* **2008**, *350*, 717−730.
(18) Tagata, T.; Nishida, M. *J. Org. Chem.* **2003**, *68*, 9412−9415.
(19) Bedford, R. B.; Singh, U. G.; Walton, R. I.; Williams, R. T.; Davis, S. A. *Chem. Mater.* **2005**, *17*, 701−707.
(20) Djakovitch, L.; Koehler, K. *J. Am. Chem. Soc.* **2001**, *123*, 5990−5999.
(21) Chen, X.; Hou, Y.; Wang, H.; Cao, Y.; He, J. *J. Phys. Chem. C* **2008**, *112*, 8172−8176.
(22) Burton, P. D.; Boyle, T. J.; Datye, A. K. *J. Catal.* **2011**, *280*, 145−149.
(23) Gao, Y.; Chen, C.-A.; Gau, H.-M.; Bailey, J. A.; Akhadov, E.; Williams, D.; Wang, H.-L. *Chem. Mater.* **2008**, *20*, 2839−2844.
(24) Bhattacharjee, S.; Bruening, M. L. *Langmuir* **2008**, *24*, 2916−2920.
(25) Kidambi, S.; Dai, J.; Li, J.; Bruening, M. L. *J. Am. Chem. Soc.* **2004**, *126*, 2658−2659.
(26) Lee, S.-S.; Park, B.-K.; Byeon, S.-H.; Chang, F.; Kim, H. *Chem. Mater.* **2006**, *18*, 5631−5633.
(27) Tanabe, K. *Mater Lett* **2007**, *61*, 4573−4575.
(28) Ebothe, J.; Kityk, I.; Chang, G.; Oyama, M.; Plucinski, K. *Physica E: Low-Dimensional Systems and Nanostructures* **2006**, *35*, 121−125.
(29) Ebothe, J.; Kityk, I.; Nzoghe-Medome, L.; Chang, G.; Oyama, M.; Sahraoui, B.; Miedzinski, R. *J. Mod. Optics* **2008**, *55*, 187−196.
(30) Balouch, A.; Umar, A. A.; Tan, S. T.; Nafisah, S.; Md Saad, S. K.; Salleh, M. M.; Oyama, M. *RSC Adv.* **2013**, DOI: 10.1039/c3ra43298j.
(31) Umar, A. A.; Oyama, M. *Appl. Surf. Sci.* **2006**, *253*, 2933−2940.
(32) Umar, A. A.; Oyama, M. *Appl. Surf. Sci.* **2006**, *253*, 2196−2202.
(33) Umar, A. A.; Oyama, M. *Cryst. Growth Des.* **2007**, *7*, 2404−2409.
(34) Umar, A. A.; Oyama, M.; Salleh, M. M.; Majlis, B. Y. *Cryst. Growth Des.* **2009**, *9*, 2835−2840.
(35) Umar, A. A.; Rahman, M. Y. A.; Saad, S. K. M.; Salleh, M. M.; Oyama, M. *Appl. Surf. Sci.* **2013**, *270*, 109−114.
(36) Umar, A. A.; Rahman, M. Y. A.; Taslim, R.; Salleh, M. M.; Oyama, M. *Nanoscale Res. Lett.* **2011**, *6*, 1−12.
(37) Umar, A. A.; Iwantono, I.; Abdullah, A.; Salleh, M. M.; Oyama, M. *Nanoscale Res. Lett.* **2012**, *7*, 1−19.
(38) Umar, A. A.; Oyama, M. *Cryst. Growth Des.* **2008**, *8*, 1808−1811.
(39) Umar, A. A.; Oyama, M. *Cryst. Growth Des.* **2009**, *9*, 1146−1152.
(40) Viñes, F.; Illas, F.; Neyman, K. M. *Angew. Chem., Int. Ed.* **2007**, *46*, 7094−7097.
(41) Yurieva, T. M. *Catal. Today* **1999**, *51*, 457−467.
(42) Shokrolahi, A.; Zali, A.; Keshavarz, M. H. *Green Chem. Lett. Rev.* **2011**, *4*, 195−203.

(43) Guella, G.; Zanchetta, C.; Patton, B.; Miotello, A. *J. Phys. Chem. B* **2006**, *110*, 17024−33.
(44) Hayes, K. S. P. M.; Mitchell, J. W.; Niak, A.; Turcotte, M. G. *Hydrogenation of Acetone*; U.S. Patent 7041857B1, May 9, 2006.